Ultrafine-Grain Structure Formation in an Al-Mg-Sc Alloy During Warm ECAP

OLEG SITDIKOV, ELENA AVTOKRATOVA, TAKU SAKAI, and KANEAKI TSUZAKI

Microstructural evolution taking place during equal-channel angular pressing was studied in a commercial Al-6Mg-0.3Sc alloy at 523 K (250 °C) (~$0.5T_m$). The structural changes are mainly associated with development of microshear bands (MSBs) that are continuously formed by strain accumulation and microstructural heterogeneities in each pass, which result in fragmentation of coarse original grains. New ultrafine grains (UFGs) with moderate-to-high angle boundary misorientations are concurrently evolved in the interiors of MSBs accompanied by rigid body rotation at medium-to-large strains. Such strain-induced grain refinement process occurs very slowly and incompletely in the present heavily alloyed Al alloy, leading to formation of a mixed microstructure, *i.e.*, the UFGs in colony and some weakly misoriented fragments of original grains. The microstructure evolved at $\varepsilon \approx 12$ is characterized by a bimodal crystallite size distribution with two peaks at $d_1 \approx 0.2$ to 0.3 μm and $d_2 \approx 0.6$ to 0.7 μm, and the fraction of high angle boundaries of about 0.35 ± 0.05. The main factors promoting dynamic formation of UFGs and the effects of thermal processes on it during severe plastic deformation are discussed in detail.

DOI: 10.1007/s11661-012-1438-4

I. INTRODUCTION

DURING the last decade, the fabrication of bulky ultrafine-grained (UFGed) structural materials by severe plastic deformation (SPD) has been one of the hottest subjects in the materials research field.[1–33] Metallic alloys processed by SPD are composed of UFGs with sizes below 1 μm and generally exhibit enhanced mechanical, physical, and chemical properties, which can be successfully utilized in commercial applications.[3,9,20,28] Several SPD techniques, such as equal channel angular pressing (ECAP),[1,3–8,10,13–16,18–21,23–26,29,31–33] accumulative roll bonding (ARB),[2,12] and multi-directional forging (MDF)[1,3,9,11,17,22,27,30] are mostly used for development of UFGed structures in numerous metals and alloys. These SPD techniques can also be a very valuable scientific tool for studying the microstructural development taking place during SPD.[1,4–8,11,15–33]

The characteristics of SPD methods and bulky UFGed materials produced currently have reasonably been well known. Fine-grained Al alloys among the materials with high stacking fault energy have been frequently studied on the processing and their properties at low-to-high temperatures.[4–6,8,10,12–21,23–26,29–33] It has been well understood that strain localization taking place in some Al alloys during SPD can result in significant intrinsic structure instability and lead to formation of deformation bands such as microshear bands (MSBs) at relatively low strains.[16,17,19,22,24–27,30,31,33] Their number and boundary misorientation increase with deformation, finally followed by a full development of fine-crystalline assemblies at high strains. Such a evolution mechanism of UFGed microstructure is often discussed as continuous dynamic recrystallization (cDRX).[11,17,22,27,34,35] The exact mechanisms of new grain formation, however, remain unclear yet, despite considerable studies being conducted on the development of UFGed structures. For instance, it has been emphasized in the recent studies[7,15,16,19–21,32] that our understanding of the processes occurring during severe deformation is still very superficial, and there have been widespread discussions regarding the grain refining mechanisms operating during SPD. This may be related to the fact that many important data regarding the microstructural development and various factors affecting grain refinement during SPD are still lacking, especially for heavily alloyed Al alloys.

It is also not clear how the processing conditions, such as deformation temperature, strain rate, deformation mode, *etc.*, affect the UFG development during SPD. In particular, increasing in deformation temperature is normally shown in some studies on low-to-moderately alloyed Al alloys to retard the formation of UFG microstructures.[5,8,10,26,31] This can be attributed to relaxation of strain compatibility between grains owing to more rapid operation of dynamic recovery at higher temperatures and less frequent development of deformation bands.[26,31,36,37] On the other hand, thermally activated processes through dynamic recovery may be

OLEG SITDIKOV, Senior Research Associate, and ELENA AVTOKRATOVA, Research Associate, are with the Institute for Metals Superplasticity Problems, Russian Academy of Sciences, Khalturina 39, Ufa 450001, Russia. Contact e-mail: sitdikov@nm.ru TAKU SAKAI, Professor, is with UEC Tokyo (the University of Electro-Communications), Chofu, Tokyo 182-8585, Japan. KANEAKI TSUZAKI, Professor, is with the National Institute for Materials Science, Tsukuba 305-0047, Japan.

Manuscript submitted September 2, 2011.
Article published online September 26, 2012

very important for development of new fine grains during cold-to-warm SPD.[22,23] It has been reported for some high strength and heavily alloyed Al alloys[30] that strain-induced high-angle boundary (HAB) formation may occur less readily at relatively low processing temperatures. Thus, temperature effect on development of strain-induced grain structures during SPD may be different for different materials and the role of dynamic recovery operated in this process have been not comprehensibly studied in sufficient details.

The aim of the current study is to investigate the microstructural evolution during warm ECAP of an Al-Mg-Sc alloy. It has been shown in the previous study[29] that the kinetics of grain refinement in this alloy is gradually accelerated with increasing processing temperature from 0.5 to $0.8T_m$, where T_m is the melting point of aluminum. In the current study, the evolution process of strain-induced grain structure was analyzed in detail during ECAP at moderate temperatures of about $0.5T_m$ and discussed comparing with that taking place at high temperature of about $0.8T_m$.[23] The starting material was a pre-extruded rod with a partially recrystallized microstructure resulted from previous extrusion and annealing operations; that may be a most suitable object for investigations of the microstructural changes during ECAP under industrial conditions. The role of thermal processes in evolution of UFGed structure during SPD is discussed in details.

II. EXPERIMENTAL PROCEDURE

The alloy used had the following chemical composition (wt pct): 6Mg, 0.4Mn, 0.3Sc, 0.2Si, 0.1Fe, and the balance Al. It was fabricated by casting into a steel mold at the Kamensk-Uralsk Metallurgical Works (Russia) and then homogenized at 793 K (520 °C) for 48 hours. Extrusion was performed at 663 K (390 °C) to a strain of about 0.7, followed by annealing at 673 K (400 °C) for 1 hour. The alloy was composed of partially recrystallized equiaxed grains with the average size of 4.4 μm and a volume fraction of about 0.35 developed along the boundaries of coarse elongated grains lying parallel to the extrusion axis (Figure 2(a)). The sizes of these coarse grains were varied from 150 to 200 μm and from 50 to 100 μm in longitudinal and transverse directions, respectively. Nano-scale dispersion particles in the present material were identified as coherent Al_3Sc dispersoids having a size from 10 to 20 nm.[23,24]

Samples used for ECAP were machined parallel to the extrusion axis into rods with a diameter of 20 mm and a length of about 100 mm. ECAP was carried out from 423 K to 523 K (from 150 °C to 250 °C) (from 0.46 to $0.56T_m$) using a circular die in cross-section with a diameter of 20 mm. The die had a channel in L-shaped configuration with an angle of 90 deg between the two channels and an angle of 0 deg at the outer arc curvature at the point of intersection. These angles lead to a strain of about 1 in each passage through the die. A heating jacket was put on the die, and the pressing temperature was controlled within ±5 K (5 °C) of the temperature range from 423 K to 523 K (from 150 °C to 250 °C). Samples were pressed repeatedly using route A, *i.e.*, the orientation of billet was not changed at each pass. The route A can be the most effective one for formation of fine-grained structure with HABs and so has been used in the author's previous studies[23–26,29,31] and applied here to provide some compatible data. Moreover, this is the simplest method of ECAP and, hence, it can be most suitable for grain refinement under industrial conditions. The ECAP was performed in a hydraulic press operating at a pressing speed of ~6 mm s^{-1}. The samples pressed were quenched in water after each deformation pass and then reheated at the ECAP temperature during 45 minutes before subsequent ECAP. More details on this procedure are represented in Reference 24.

After five and exceptionally six passes at 423 K (150 °C), severe macrocracks were evolved parallel to the shear plane at the L-shaped corner with spacing about 3 to 5 mm from each other. ECAP at above 473 K (200 °C) was successfully performed up to 12 passes. Samples after ECAP were cut from central places of the pressed rods in longitudinal section parallel to the pressing direction (PD) for microhardness measurements and various microstructure observations, such as optical microscopy, electron back scattering diffraction pattern (EBSP), and transmission electron microscopy (TEM) analyses. The Vickers hardness was measured at room temperature with a load ranging from 0.5 to 1 N. Metallographic observations were carried out using a Nikon L-150 optical microscope and scanning electron microscope (SEM) JSM-840 after etching with a standard Keller's reagent. (Sub)grain boundary misorientation distributions were obtained from EBSP using JSM-6500 SEM equipped with a field-emission gun. Over the misorientation parameters measured by EBSP, the boundaries with misorientation less than 2 deg were not taken into account. Specimens for TEM examination were mechanically ground to a thickness of about 200 μm and electro-polished at 20 V in a solution of 30 pct HNO_3 and 70 pct CH_3OH at a temperature of 243 K (−30 °C) using a Tenupol-3 twin-jet polishing unit. They were then examined using a JEOL-2000EX TEM. The mean (sub)grain size was measured by the line-intercept method.

III. EXPERIMENTAL RESULTS

A. *Room-Temperature Hardness*

Changes in Vickers hardness with ECAP from 423 K to 523 K (150 °C to 250 °C) are summarized in Figure 1. The hardness change after ECAP at 723 K (450 °C)[23] is also represented in Figure 1 for comparison. It is seen that hardness increases with ECAP at T = 423 K to 523 K (150 °C to 250 °C) and reaches higher values after ECAP at lower temperatures. The shape of the HV-ε curves suggests a remarkable hardening taking place at earlier stages of ECAP (ε = 1–2) followed by a decrease in the hardening rate after subsequent processing (ε = 2–4) and finally approaching

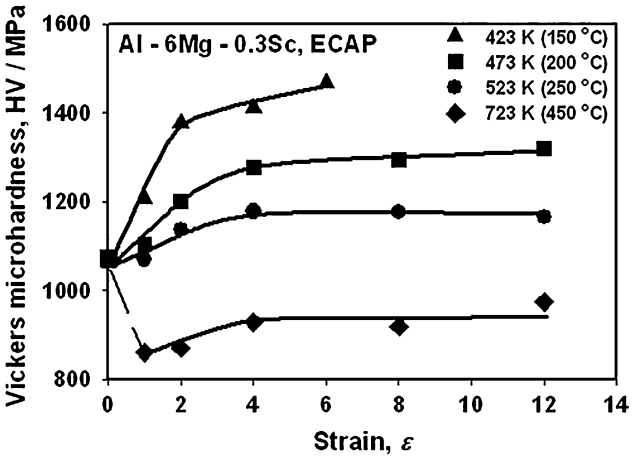

Fig. 1—Hardness changes in Al-6Mg-0.3Sc alloy after ECAP in the temperature interval from 423 K to 723 K (from 150 °C to 450 °C).

constant hardening rates at higher strains ($\varepsilon \geq 4$). The rate of hardening gradually decreases and approaches zero in high strain at 523 K (250 °C). It is noted that such attenuating strain hardening behavior of the microstructures produced by warm ECAP can be comparable with that of some cubic materials processed by SPD and may be typical of plastic deformation in severe high strain at low-to-intermediate temperatures.[11,22] This suggests that deformation during warm ECAP can be controlled by dynamic recovery.[34] Such a temperature effect on the hardening behavior may be attributed to acceleration of the rate of dynamic recovery controlling structural changes.

It is seen in Figure 1, on the other hand, that the hardness at 723 K (450 °C) drops discontinuously from 1070 MPa to about 850 MPa just after first ECAP pass. Then the hardness at $\varepsilon > 1$ increases with ECAP in low strain and approaches a saturation value in high strain at $\varepsilon \geq 4$. This behavior is roughly similar to those between 473 K and 523 K (between 200 °C and 250 °C). A discontinuous decrease in hardness after first pressing at 723 K (450 °C) may result from the reason that high density dislocation microstructures developed during previous extrusion at 663 K (390 °C) may be decreased and rearranged by dynamic recovery operating during first ECAP pass at 723 K (450 °C). This is described in detail elsewhere.[23]

B. *Deformation Microstructures*

A series of typical microstructures (a) before ECAP ($\varepsilon = 0$) and (b) through (d) after ECAP to $\varepsilon = 1$ to 12 at 523 K (250 °C) are represented in Figure 2. It is remarkable to see that the deformed microstructures developed after first passage are mainly characterized by elongated coarse grains aligned roughly parallel to the PD and concurrently deformation bands are frequently and heterogeneously formed in their interiors (Figure 2(b), see also Figure 3(a)). These bands evolved in aluminum alloy are found to be mainly MSBs, the characteristics of which are described elsewhere.[16,17,22,25–27,30,31,33,34,37] Their density remarkably increases with further deformation to $\varepsilon = 4$ (Figure 2(c)). Several sets of such bands are developed in various directions, as can be seen at larger magnification in Figure 2(d). The latter may be consistent with various shearing orientations appeared in route A at this ECAP strain.[20,21] It is also evident that MSBs intersect each other resulting in a spatial net within original grains, and concurrently, new UFGs frequently evolve in the interiors of MSBs, as indicated by arrows in Figure 2(d). The current study's data suggest that repeated shearing during ECAP can lead to formation of MSBs and play important role for strain-induced formation of submicrocrystalline structures upon severe warm working, as discussed later. After sufficiently large amount of strains ($\varepsilon = 8$ to 12), MSBs and new fine crystallites are more homogeneously developed in the whole volume of the ECAPed samples (Figure 2(e)). Such a microstructural development will be discussed later in more detail using high-resolution EBSP and TEM.

Typical orientation imaging microscopy (OIM) microstructures developed at (a) $\varepsilon = 1$ and (b) $\varepsilon = 2$ are depictured in Figure 3. In these OIM maps, the different gray-scale levels indicate the different crystallographic orientations, and the differences between neighboring grid points $5 \text{ deg} \leq \theta < 15 \text{ deg}$ and $\theta \geq 15$ deg are marked by narrow gray and bold black lines, respectively. Figures 3(c) and (d) show in turn typical distributions of point-to-point ($\Delta\theta$) and cumulative point-to-origin ($\Sigma\Delta\theta$) misorientations developed along the test lines T_1 and T_2 indicated in Figures 3(a) and (b). The values of $\Delta\theta$ and $\Sigma\Delta\theta$ define the misorientations evolved by 0.15 μm step relative to the previous point and the first point, respectively. It is seen in Figures 3(a) and (c) that deformation substructures develop very non-uniformly at $\varepsilon = 1$. Misorientation changes along the line T_1 show that rather straight low-angle boundaries (LABs) are frequently formed across grain interiors. Most of them have misorientations less than 3 to 5 deg and so are not sharply defined, while significant orientation gradients are evolved in coarse grain interiors. At the same time, more intense subboundaries with misorientations $\Delta\theta$, ranging from 5 to 10 deg can be observed in some local areas mostly adjoining to the mantle regions and being oriented to the PD at the angle α of about 45 deg. Cumulative misorientations change discontinuously in these regions and may correspond to the dislocation subboundaries of embryos of MSBs,[25,31] which will be discussed latter.

With further deformation to $\varepsilon = 2$ (Figures 3(b) and (d)), the number and misorientation angle of such embryos of MSBs increase, and they are progressively transformed into macroscopic long-distance MSBs. Their boundary misorientations may become over 10 to 20 deg at $\varepsilon = 2$. The angle of the MSBs with respect to the PD decreases significantly with repeated ECAP (from 45 to 18 deg). This suggests that MSBs have a persistent nature of the microstructure and, once formed, are progressively reoriented by further ECAP in route A.[16] It is also remarkable to see that new UFGs with moderate-to-high angle boundary misorientations have now started to evolve in chains in some

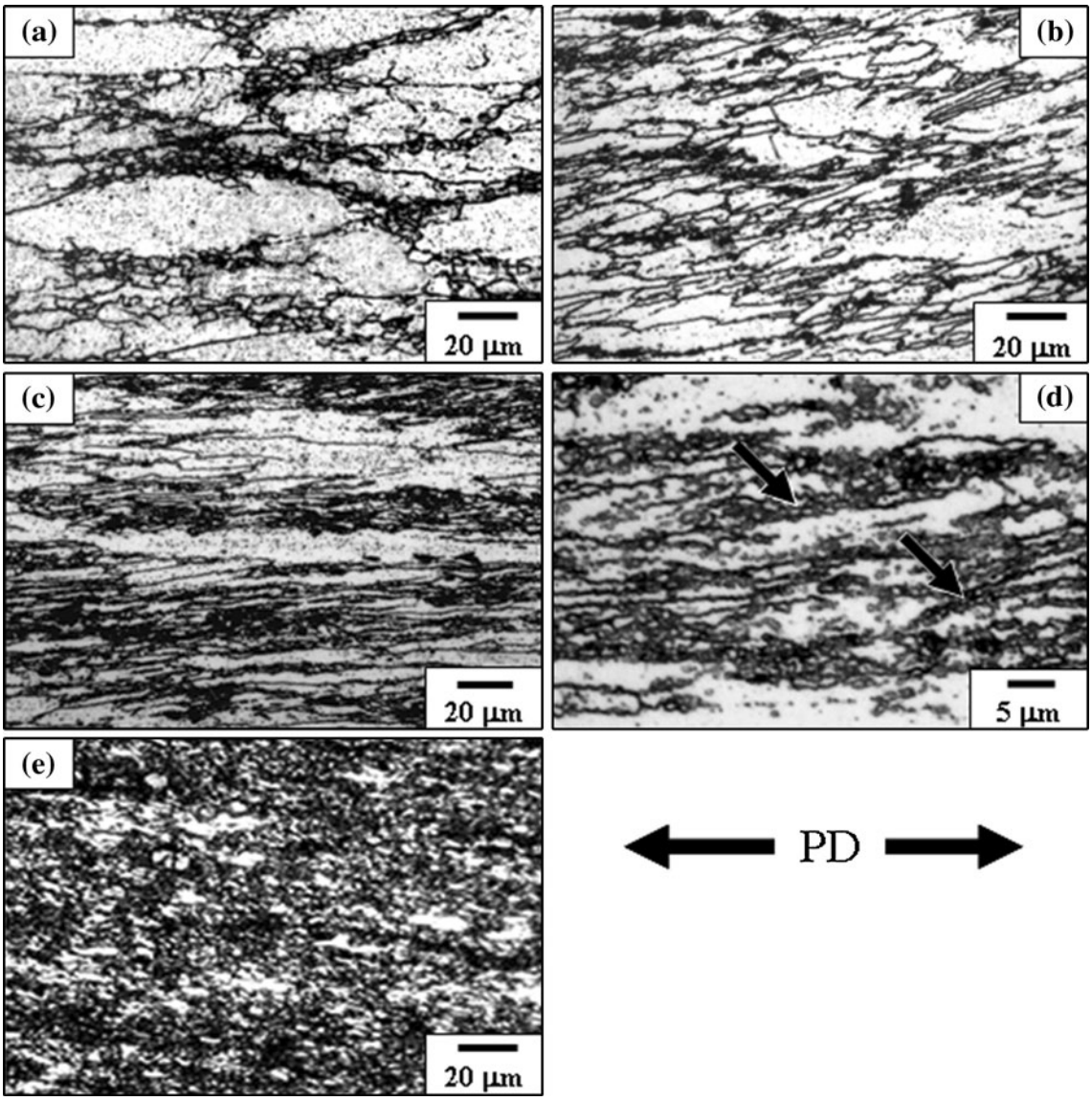

Fig. 2—Typical OM microstructures developed during ECAP at 523 K (250 °C) in Al-6Mg-0.3Sc alloy: (*a*) $\varepsilon = 0$ (before ECAP), (*b*) $\varepsilon = 1$, (*c*) and (*d*) $\varepsilon = 4$, and (*e*) $\varepsilon = 12$. Dark regions are composed of ultra-fine grains evolved. PD is the pressing direction. As seen in (b) and (c), after the second and the fourth passes in route A, the alignment angles of the elongated grains with respect to the PD are about 26.5 and 7.2 deg, respectively.[7]

places of MSBs in grain interiors and in grain-boundary regions, respectively, as arrowed in Figure 3(b).

Figure 4(a) shows a typical OIM map of the deformation structure evolved at $\varepsilon = 4$, and Figures 4(b) and (c) show the associated point-to-point and cumulative misorientations measured along the lines T_3 and T_4, respectively. It is seen in Figure 4(a) that several sets of MSBs with moderate-to-high angle boundary misorientations are developed in various directions accompanied with evolution of UFGs, *e.g.*, as denoted by the line T_4. The intersections of MSBs are accompanied by the evolution of relatively coarse flattened fragments of original grains, and so UFGs are partially and inhomogeneously evolved in several places. The observations that have particular relevance to the current description of structural changes in these local places can be described as follows:

(i) The crystallites formed at $\varepsilon = 4$ are bounded by rather sharp (sub)boundaries, many of which have high-angle misorientation, as denoted by point-to-point misorientations developed along the line T_4 (Figure 4(c)).
(ii) The cumulative misorientation is alternatively restored in the same places along the line T_4; that testifies that the fragmented regions may maintain a similar crystallographic orientation during ECAP.

On the other hand, the dislocation subboundaries in some coarse remnant grains that are located far from the extensive microshear intersection are still diffuse in the image and bear low-to-moderate angle misorientations, as indicated by the line T_3 in Figure 4(b). This

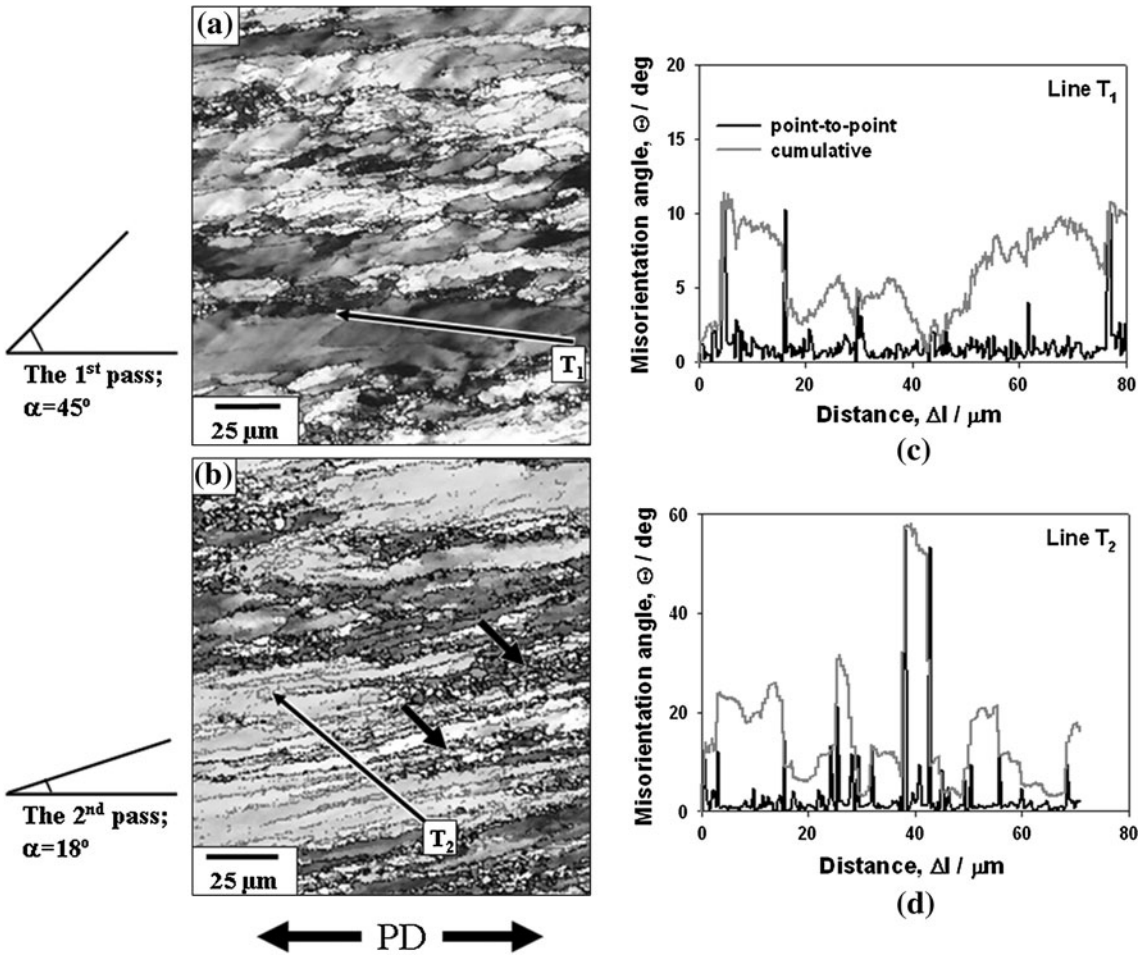

Fig. 3—Typical OIM microstructures developed during ECAP of Al-6Mg-0.3Sc alloy at 523 K (250 °C): (*a*) $\varepsilon = 1$, (*b*) $\varepsilon = 2$. The (*c*) and (*d*) show the typical misorientations developed along the lines T_1 and T_2 indicated in (a) and (b), respectively. PD is the pressing direction.

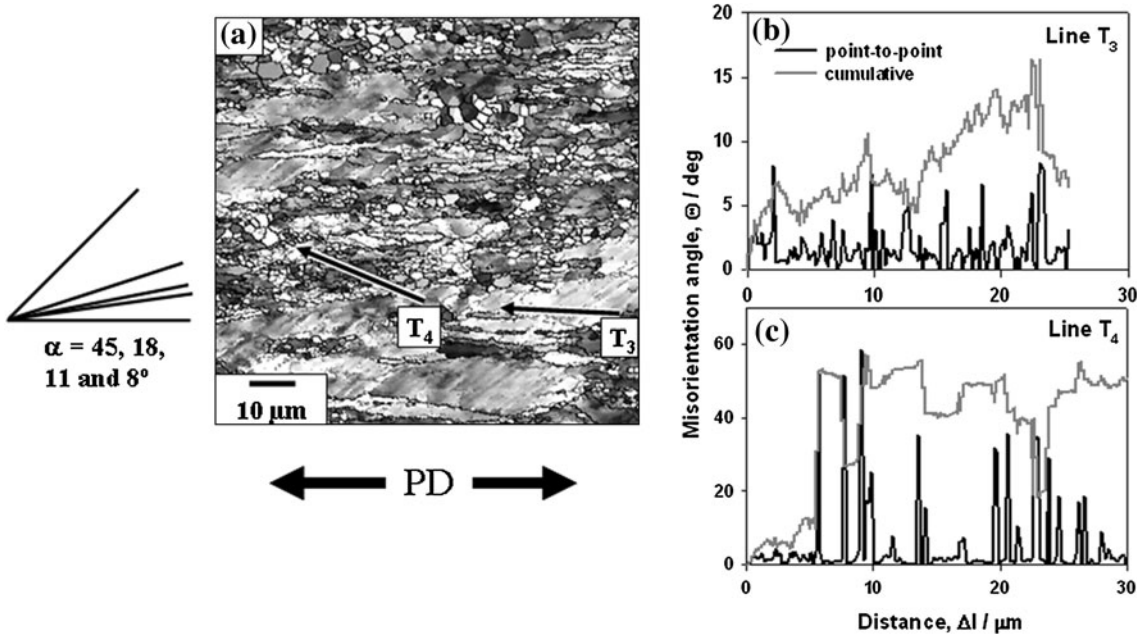

Fig. 4—(*a*) Typical OIM microstructure developed at $\varepsilon = 4$ during ECAP of Al-6Mg-0.3Sc alloy at 523 K (250 °C). (*b*) and (*c*): The typical misorientations developed along the lines T_3 and T_4 indicated in (a). PD is the pressing direction.

supports the assumption[27] that MSB intersections can be preferential sites for the development of highly misoriented submicrocrystalline structure. It is also interesting to note in Figure 4 that the angle of such diffuse boundaries developed in coarse grains is roughly 45 deg with respect to the PD even after four ECAP passes, while that for MSBs decreases significantly, as described in Figure 3. This suggests that the former may have a temporal nature and, in contrast, the latter—a persistent one.

Figures 5(a_1) and (a_2) show typical OIM pictures of different places in the present Al alloy ECAPed to $\varepsilon = 12$. It is seen that the microstructure represented in Figure 2(e) remains actually inhomogeneous on a mesoscopical level even at $\varepsilon = 12$ and is composed by both UFGs with HABs and rather coarse fragmented parts of original grains. Even if the microstructures existed in coarser remnant grains are excluded (Figure 5(a_2)), the microstructures developed in intersection of MSBs (Figure 5(a_1)) are characterized by a bimodal crystallite size distribution with two peaks at $d_1 \approx 0.2$ to 0.3 μm and $d_2 \approx 0.6$ to 0.7 μm, as shown in Figure 5(b). The ultrafine crystallites that correspond to d_1 may be largely misoriented equiaxed grains and develop in MSBs by large strain deformation. The volume fraction of such structural component, however, is still small even at $\varepsilon = 12$ and does not exceed 0.4. In contrast, the coarser crystallites with d_2 in Figures 5(a_1) and (a_2) contain frequently low-to-moderate dislocation subboundaries in their interiors and incorporate the following distinctive features; that is, they have some irregular shape and ragged grain boundaries, and exhibit a similar crystallographic orientation of the closely located grains, as confirmed by the OIM grayscale contrast. Referring to such a microstructural evolution described above in Figures 2 through 5, it is safety to assume that these crystallites are the parts of original grains lying in exteriors of MSBs.

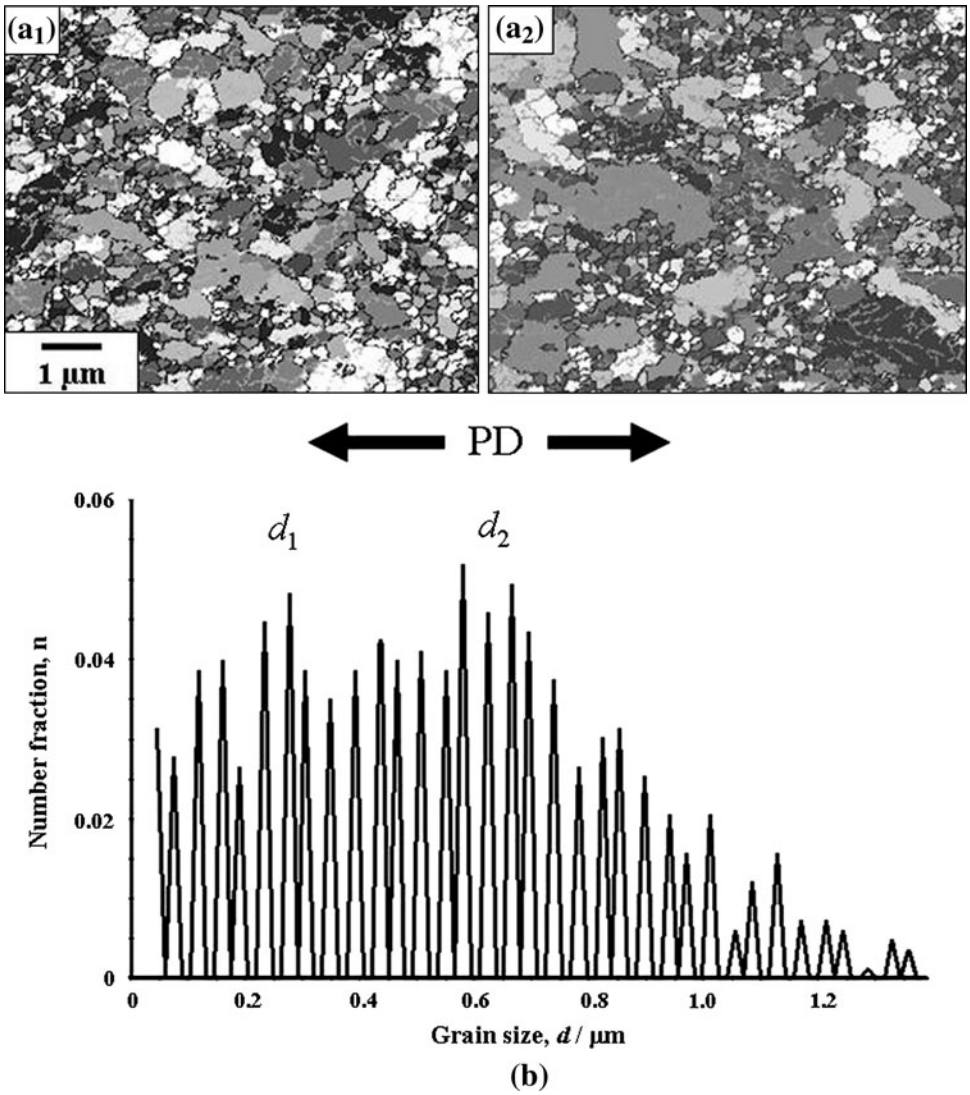

Fig. 5—(a_1) and (a_2) Typical OIM microstructures developed at $\varepsilon = 12$ during ECAP of Al-6Mg-0.3Sc alloy at 523 K (250 °C); PD is the pressing direction. (*b*) Typical distribution of the (sub)grain size developed in fine-grained regions. The data are derived from the high-resolution EBSP analysis with the scanning step size of 25 nm.

C. *TEM Microstructures*

It has been shown in the previous studies on the present Al alloy[23,24] that the preliminary warm-to-hot thermo-mechanical treatment before ECAP (Section II) results in formation of a well-developed (sub)grain structure with an average crystallite size of about 1.6 μm. Figure 6 represents the typical TEM microstructures and selected area electron diffraction (SAED) patterns for the samples ECAPed to ((a) and (b)) $\varepsilon = 1$, and ((c) and (d)) $\varepsilon = 4$ at 523 K (250 °C). The objective apertures of 10 μm in diameter were employed for SAED analysis. During ECAP carried out at $\varepsilon = 1$ (Figures 6(a) and (b)), original subgrain microstructure is gradually replaced by a new finer subgrain/cell band structure, which is composed by equiaxed subgrains as well as elongated crystallites separated by dislocation subboundaries with low-to-moderate angle misorientations. These are noted by the SAED patterns inserted in Figure 6(a). Most of subgrains/cells in this structure contain a relatively low density or almost free dislocations after first ECAP pass. It is also seen in Figure 6(b) that diffuse linear dislocation walls observed are not fully condensed and composed of individual dislocations. They are also frequently terminated into areas of more homogeneous dislocation distribution. After ECAP to moderate-to-high strains ($\varepsilon = 4$), in contrast, substructures with higher density dislocations are developed in some areas, as shown in Figures 6(c) and (d). These show elongated cell- and banded substructures with some regions containing almost free lattice dislocations in cell/subgrain interiors. As seen in Figure 6(d), dislocation densities in such regions may be often so high that separate lattice dislocations can hardly be resolved by TEM technique. Note that directional dislocation subboundaries evolved in these regions are still diffuse and have low misorientations that may be consistent with the banded features in remnant original grains indicated by the line T_3 in EBSD maps in Figure 4.

Figure 7 represents the typical features of the distribution of high density lattice dislocations and secondary phase dispersion particles in such areas at a strain of 4. It is seen in Figure 7(a) that the spatial distribution of the dispersion particles in the deformed structure is nearly homogeneous, and some of them demonstrate a well-known "coffee-bean"-like contrast, which can be attributed to the coherent dispersoids.[16,23,24] Hence, they can be clearly recognized as the coherent $L1_2$-Al_3Sc particles (Section II). It is important to note that the size of these particles is unaltered during ECAP at 523 K (250 °C) and is about 10 to 20 nm. Also, there is a high density of lattice dislocations associated with the dispersoids, as shown in Figure 7(b). Note here that a strong dislocation-dispersoid interaction frequently takes place in the earlier stages of deformation, as it is evident in Figure 6(b). This suggests that the dispersoids can trap the dislocations, significantly inhibiting

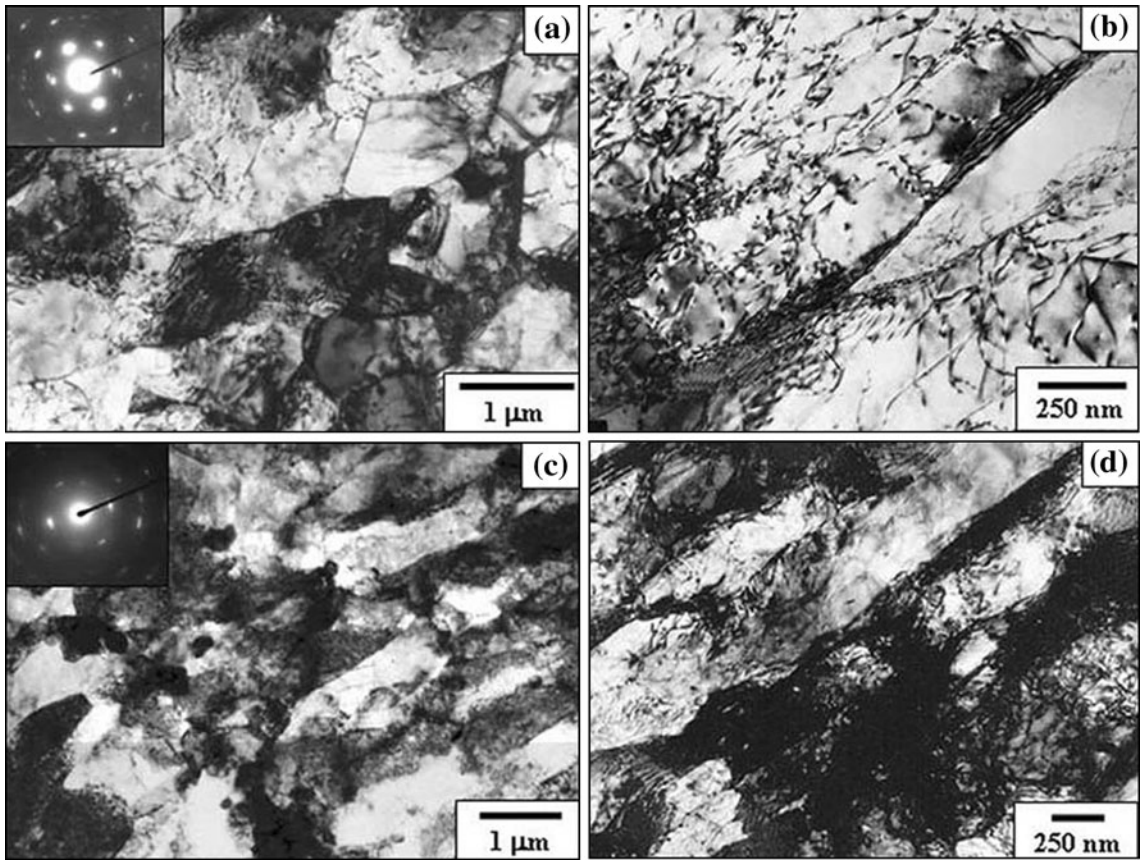

Fig. 6—Typical TEM microstructures developed during ECAP of Al-6Mg-0.3Sc alloy at 523 K (250 °C): (*a*) and (*b*) $\varepsilon = 1$, (*c*) and (*d*) $\varepsilon = 4$.

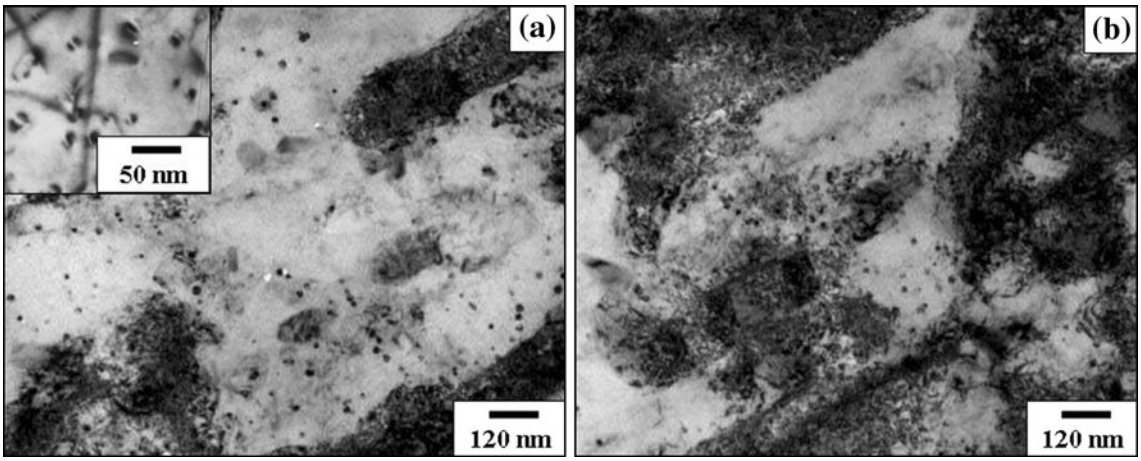

Fig. 7—Typical TEM micrographs showing the distribution of high density lattice dislocations and dispersoid precipitates in the structures developed during ECAP of Al-6Mg-0.3Sc alloy at 523 K (250 °C) and $\varepsilon = 4$.

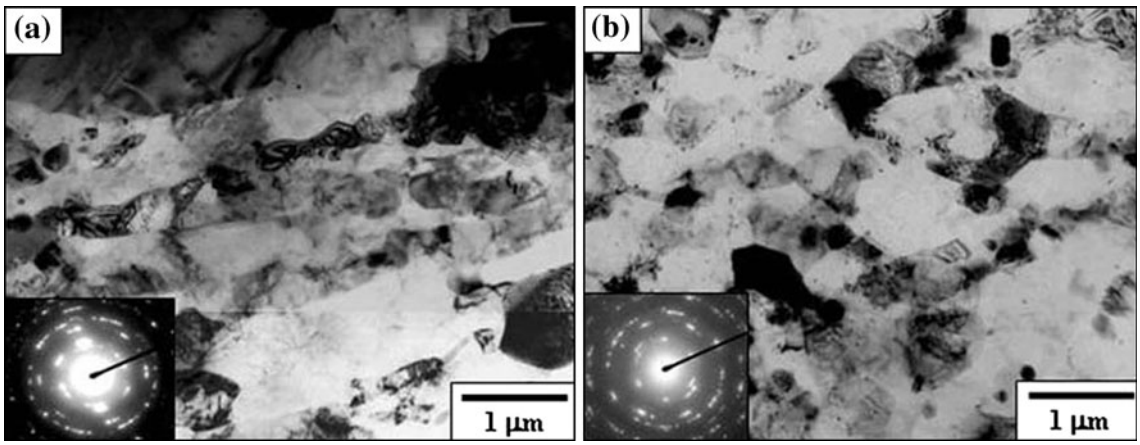

Fig. 8—Typical TEM microstructures developed during ECAP of Al-6Mg-0.3Sc alloy at 523 K (250 °C): (*a*) $\varepsilon = 4$, (*b*) $\varepsilon = 12$.

recovery even at elevated temperatures and thus promoting "diffuse" dislocation substructures.

Some typical examples of the deformation microstructures developed in the areas fragmented by mutually intersected MSBs in high strains ($\varepsilon = 4$ and $\varepsilon = 12$) are represented in Figure 8. It is remarkable to see that directional microcrystallines (Figure 8(a)) and roughly equiaxed UFGs with HABs (Figure 8(b)) are evolved at $\varepsilon = 4$ and $\varepsilon = 12$, respectively. These show the regions outlined by boundaries with moderate-to-high angle misorientations, as suggested by the enclosed ring-like diffraction patterns. It is seen that these strain-induced submicrocrystalline structures involve the bands of equiaxed UFGs that are developed preferably at the intersections of MSBs and have a remarkably finer size as compared with that of other crystallites outside the bands (compare Figures 6 and 8). Some of such UFGs are bonded by sharp grain boundaries with distinct extinction fringes, which are typical of ordinary grain boundaries in recrystallized microstructure. The fractional increase in the UFGed regions with increase in strain from $\varepsilon = 4$ to 12 (Figures 2(c) and (e)) results from an increasing number of intersections of MSBs by subsequent ECAP and some expansion of the volume of UFGs formed.

Strain dependence of the mean (sub)grain size measured in a whole volume is shown by full circles in Figure 9. The sizes of all crystallites were measured in both longitudinal and transverse directions and then averaged at each strain. The average size of UFGs developed in the interiors of MSBs is also represented by open circles in Figure 9. It is seen that the (sub)grain size measured in a whole volume rapidly decreases from 1.6 to 1.1 μm with pressing to $\varepsilon = 4$ and then approaches a roughly constant value of about 0.8 to 0.9 μm in high strain. In contrast, the size of UFGed component developed in MSBs remains essentially constant in medium-to-high strain and is about 0.2 to 0.3 μm.

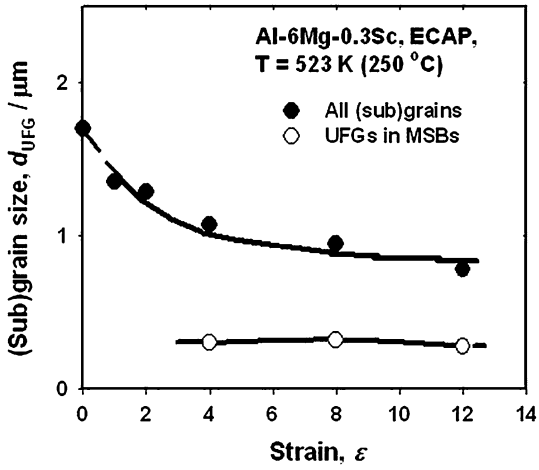

Fig. 9—Changes in the size of (sub)grains developed during ECAP at 523 K (250 °C).

These TEM data can provide an independent evidence that the UFG microstructure with two different (sub)-grain size is evolved at high strains in the current Al alloy.

D. *Misorientation Characteristics of the Evolved Microstructure*

Figure 10 shows the misorientation distributions of the strain-induced (sub)boundaries that were selected in a whole area in the deformation substructures evolved at (a) $\varepsilon = 0$; (b) $\varepsilon = 1$; (c) $\varepsilon = 4$, and (d) $\varepsilon = 12$. It is seen in Figure 10(a) that most of boundaries in the initial microstructure, *i.e.*, at $\varepsilon = 0$, exhibit low-to-medium angle misorientations from 5 to 15 deg, as well as those above 15 deg, which were mainly developed by pre-treatment before ECAP.[23,24] After first ECAP pass (Figure 10(b)), the average misorientations, Θ_{ave}, and the fraction of high-angle boundaries, f_{HABs}, decrease from 18.7 to 13.7 deg and from 0.41 to 0.27, respectively, which may be related to formation of new LABs (Figure 6). With further straining, the fraction of low-to-moderate angle boundaries somewhat decreases and spreads out toward the larger misorientations, as shown in Figures 10(c) through (d); this may be directly connected with the formation of MSBs and new UFGs. It is remarkable to see, however, that this process occurs very slowly in the present heavily alloyed Al alloy at 523 K (250 °C), as it can be compared, for instance, with a moderately alloyed Al-Cu alloy ECAPed at similar deformation conditions[25] or the same Al-Mg-Sc alloy deformed at higher temperature,[23] in which larger fractions of high-angle boundaries are eventually evolved at high ECAP strains. In contrast, the histograms plotted for the present Al-Mg-Sc alloy even at $\varepsilon = 12$ show the relative abundance of LABs with only one well-defined peak located at low misorientations <5 deg and a roughly flat misorientation distribution for the boundaries ranging from 15 to 60 deg (Figure 10(d)).

Strain dependencies of the Θ_{ave} and f_{HABs} at 523 K (250 °C) are represented by a solid line with full circles

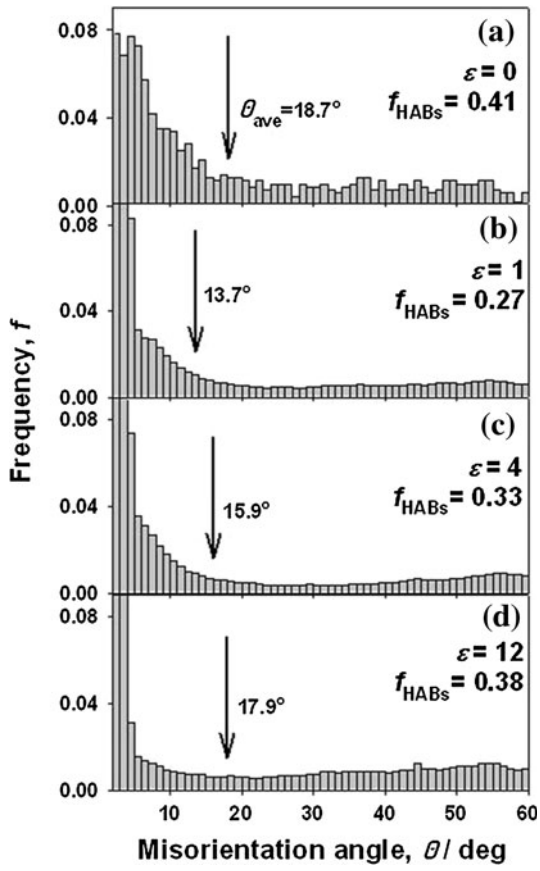

Fig. 10—Changes in misorientation distribution of dislocation and (sub)grain boundaries developed with repeated ECAP in Al-6Mg-0.3Sc alloy at 523 K (250 °C): (*a*) $\varepsilon = 0$, (*b*) $\varepsilon = 1$, (*c*) $\varepsilon = 4$, and (*d*) $\varepsilon = 12$.

in Figures 11(a) and (b), respectively. The data for the same alloy obtained at 723 K (450 °C)[23] are also plotted by a dashed line with open circles for comparison. It is seen that the Θ_{ave} and f_{HABs} at 523 K (250 °C) first drop to the minimum values of 14.2 deg and 0.26 at $\varepsilon = 1$ to 2 and then grow with increasing strain from 2 to 4, followed by a saturation of about 17 ± 1 deg and 0.35 ± 0.05 in high strain, respectively. In contrast, both the Θ_{ave} and f_{HABs} evolved at 723 K (450 °C) continuously increase with ECAP in low-to-high strain, approaching significantly larger values of 34.5 ± 1 deg and 0.80 ± 0.05 at $\varepsilon = 12$, respectively. It is evident in Figure 11, thus, that the kinetics of grain refinement in the present Al-Mg-Sc alloy can be significantly accelerated with increasing ECAP temperature ranging from 523 K to 723 K (from 250 °C to 450 °C).

E. *Texture*

Figure 12 shows typical inverse pole figures of the PD derived from EBSD analysis, which were plotted in fine-grained regions in the Al-Mg-Sc alloy developed at $\varepsilon = 12$ during ECAP between 523 K and 723 K (250 °C and 450 °C). It is seen in Figure 12(a) that a rather strong fiber texture is evolved at 523 K (250 °C), in which a maximum of the orientation density tends to

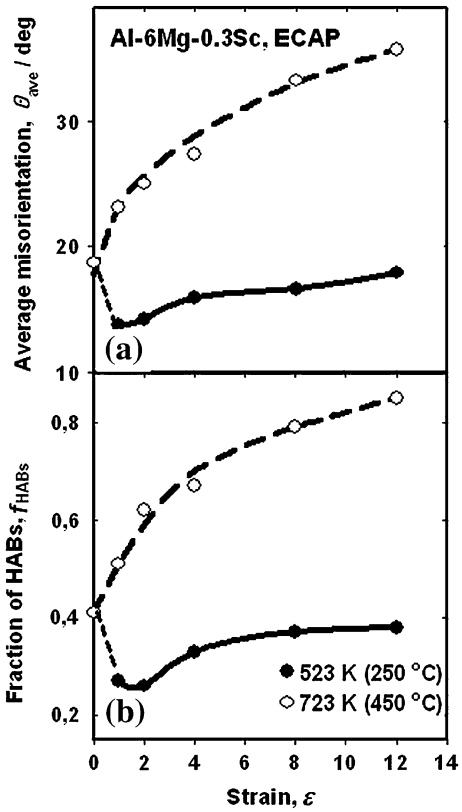

Fig. 11—Effect of warm-to-hot ECAP on: (*a*) the average misorientation of dislocation/(sub)grain boundaries, Θ_{ave}, and (*b*) the fraction of HABs, f_{HABs} developed during ECAP of Al-6Mg-0.3Sc alloy at 523 K (250 °C). The data at 723 K (450 °C) for the same alloy[23] are shown by dashed lines with open circles for comparison.

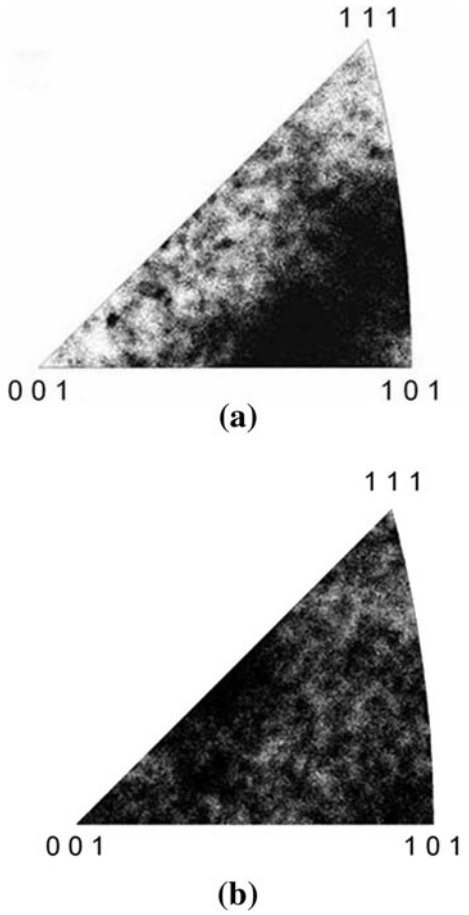

Fig. 12—Typical inverse pole figures showing textures evolved in fine-grained regions in Al-6Mg-0.3Sc alloy during ECAP to $\varepsilon = 12$ at (*a*) 523 K (250 °C), (*b*) 723 K (450 °C).

approach ⟨101⟩ direction. Additionally, broad bands of orientations fill the whole range along the line from ⟨001⟩ to ⟨111⟩; that may be comparable to the structural changes occurring during cold rolling.[38] Such a result in the present Al alloy can be related to the mixed microstructure with the $f_{HABs} \sim 0.4$ and the $\Theta_{ave} \sim 18$ deg evolved at 523 K (250 °C) (Figure 11). The inverse pole figure evolved at 723 K (450 °C) shows, in contrast, a roughly random texture (Figure 12(b)). Such a remarkable change in texture evolved during ECAP at 723 K (450 °C) may result from more extensive (sub)grain rotation taking place at high temperature and especially in the regions of UFGs with the $f_{HABs} \sim 0.85$ and the $\Theta_{ave} \sim 35$ deg (Figure 11). This will be discussed in Section IV.

IV. DISCUSSION

A. *Evolution Process of New UFG Structure*

It is clarified in the current study that the mechanism of strain-induced grain formation may be associated with MSBs developed during ECAP. Such results may be similar to the characteristics of substructural changes and grain refinement processes taking place, for instance, during cold rolling of Al-0.1 pct Mg alloy,[39] room-temperature ECAP of Al-Mg alloys with Mg content from 0.1 to 10 pct,[16,33] warm-to-hot ECAP of Al-3 pct Cu and 2219 Al alloy[25,26,31] and during MDF at low, intermediate and high temperatures in pure copper,[22] Fe-20 pct Cr alloy[27] and 7475 Al alloy,[17,30] respectively. It has been pointed out in these studies that grain refinement process taking place during SPD may be related to evolution of MSBs, which are inhomogeneously formed by dynamic relaxation of strain gradients developed in grain interiors irrespective of various metallic materials, deformation modes, and temperatures. The microstructures developed consist of crossing MSBs, which intersect cellular and subgrain structures with high density dislocations. Contrary to cellular dislocation structures developing at the exteriors of MSBs, which have small boundary misorientation even at relatively high strains,[30] strain-induced (sub)grains are concurrently formed within MSBs during SPD primarily at the intersections and subsequently along MSBs and characterized by medium-to-high angle deformation (sub)boundaries.

Similar discussion can be applied to describe the microstructural evolution in the current Al-Mg-Sc alloy, as shown in Figures 2 through 6. In fact, the deformation substructures that appear in some grains in this alloy from 200 °C to 250 °C after the first ECAP pass

(Figure 3(a)) are (i) the well-defined banded arrays; (ii) the misorientation of their boundary segments adjoined to original boundaries is within the range from 5 to 10 deg and (iii) their crystal orientation is clearly alternated with matrix. It is believed therefore that those may be attributed to embryos of MSBs, as it is described elsewhere.[25] A model for strain-induced grain formation based on grain fragmentation by MSBs proposed in References 27, 30 may be modified to that for ECAP process, which is schematically drawn in Figure 13, and discussed as follows.

(i) During repeated ECAP process, the embryos of MSBs may be frequently introduced in an early stage of deformation parallel to the shearing plane in ECAP,[16,28], *i.e.*, at the angle of around 45 deg to the PD, and, as seen in Figures 3 and 4, changed to large-scale MSBs at higher strains.[25] MSBs may be roughly categorized as banded arrays of deformation-induced boundaries having persistent nature.[16,17,22,27,39] Hence, ones formed, they can progressively rotate with further processing in route A to establish the angles of 18, 11, and 8 deg with PD after the second, third, and fourth subsequent passes.[20,21] Also, as shown elsewhere,[19,24,25] new bands evolved in the subsequent passes intersect the previously formed ones. In Figure 13, which is represented for first four ECAP passes, the MSBs developed after the first, second and third passes are indicated as 1p, 2p and 3p, respectively.[21] Such rearrangement of the MSBs accompanied by repeated ECAP and their crossing by newly evolved MSBs (4p) can result in formation of arrays of MSBs with different orientations and, hence, promote continuous fragmentation of coarse original grains.

(ii) The crystal orientation of MSBs is considerably away from that of the adjacent matrix (Figures 3(d) and 4(c)). It is also changed discontinuously and frequently alternated at their boundaries, so that the crystal orientation of the coarser domains separated by MSBs, *e.g.*, A and B in Figure 13, seems to be not significantly changed by microshearing. This is reasonably consistent with the assumption that new UFGs with moderate-to-high angle boundary misorientations appear primarily at the intersections of MSBs, followed by their development in the interiors of MSBs, accompanied by rigid body rotation at medium-to-larger strains.[27] As new grains are evolved preferentially along MSBs, the necessary condition for a full formation of UFGed structure should be a full development of high-density MSBs in a whole volume, which can be achieved only after SPD.

(iii) It should be noted in Figure 13 that initial grain subdivision by MSBs as well as the rigid lattice rotations within these bands may be considered as some mechanically induced events, and so these events may have athermal nature.[22,26,27,31] On the other hand, the observed steady state-like hardness dependence on strain and its temperature dependence in high strain above $\varepsilon = 4$ (Figure 1) imply that dynamic recovery may play an important role in evolution of the deformation microstructure.[16,22,27,30] It is worthy to note in this connection that the boundaries of MSBs introduced by SPD are rather non-equilibrium and diffuse interfaces,[20] as observed in Figure 14. Dynamic recovery that frequently occurs at elevated temperatures can assist the transformation of such strain-induced non-equilibrium boundaries to more equilibrium ones, leading to the for-

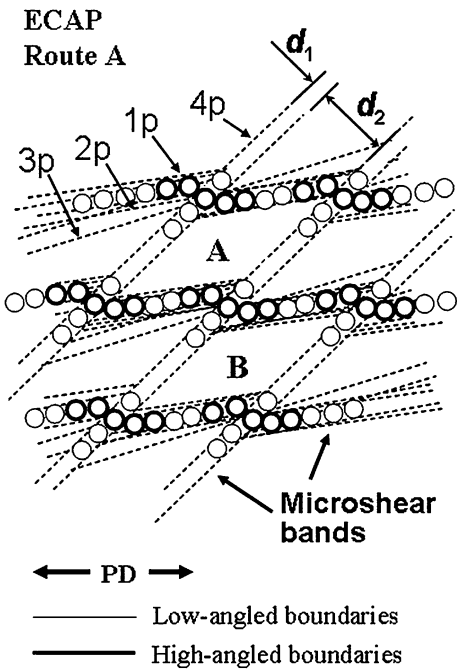

Fig. 13—Schematic drawing of the development of MSBs during ECAP and formation of new UFGs along MSBs in the regions of the rigid lattice rotation. Geometrical features of the evolution of MSBs upon four passes of ECAP by route A are represented in accordance with Refs. [20, 21]. The boundaries of MSBs evolved in each pass, *i.e.*, 1p, 2p, 3p, and 4p, are represented by dashed lines. PD is the pressing direction.

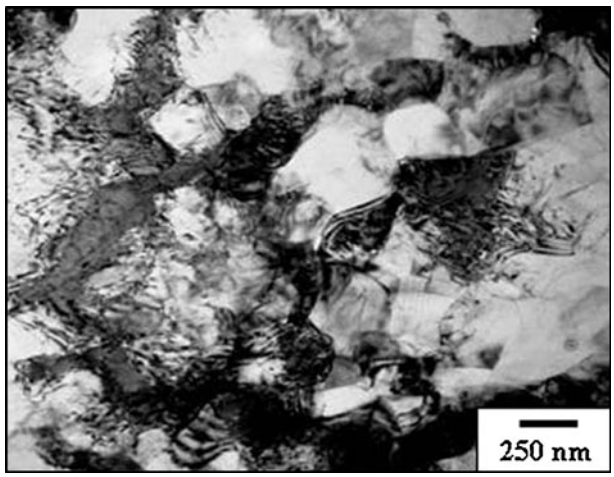

Fig. 14—Typical TEM microstructures developed during ECAP of Al-6Mg-0.3Sc alloy at 523 K (250 °C) and $\varepsilon = 12$.

mation of new UFGed structures. Repeated deformation to large strains can give enough time for dislocation rearrangement in strain-induced boundaries, leading to both an increase of grain boundary misorientation and a decrease of dislocation density in (sub)grain interiors. Thus, the formation of strain-induced grains may be controlled by dynamic formation of non-equilibrium and moderate-to-high angle boundaries at earlier stages of SPD, and subsequently by operation of dynamic recovery in these boundaries at large strains.[26] Microstructural changes at latter stages of SPD are, therefore, considered to be effectively controlled by thermally activated rate processes.[22,26]

Finally, it is important to note in Figures 9 through 11 that the fraction of HABs and the average misorientation are gradually increased by repeated ECAP accompanying with grain refinement, while the grain size of UFGs remains essentially constant at moderate-to-high strains. Such dependencies may be considered to be specific features of strain-induced grain structures, which are typical of cDRX.[11,34] It is concluded, therefore, that new fine grains evolved during warm-to-hot ECAP of the present Al alloy can be resulted from a series of strain-induced continuous reactions; that is essentially similar to cDRX.

B. *Temperature Effect on the Kinetics of Grain Refinement*

The data of the current study on the current Al-Mg-Sc alloy indicate that dynamic formation of UFGed structures occurs very slowly and incompletely even at very high strains during ECAP at 523 K (250 °C). ECAP results in formation of a mixed microstructure, which contains some weakly misoriented fragments of original grains bonded by the colonies of UFGs (Figures 5 and 8). During ECAP at 723 K (450 °C), in contrast, a rapid increase in the average boundary misorientation and the fraction of HABs takes place in the whole volume of the same alloy (Figure 11). It should be noted that such positive temperature effect on the kinetics of new grain development may be inconsistent with that for the kinetics of fine grain formation at the similar SPD conditions in low- and moderately alloyed Al alloys, *e.g.*, in pure Al,[8] Al-3 pct Cu alloy[31] and AA 2219,[26], *etc.*, in which the volume fraction and the average misorientation angle of deformation-induced grains are reduced with increasing temperature beyond the range of temperature from 523 K to 573 K (from 250 °C to 300 °C) (~0.5-0.6T_m). The possible reasons for such opposite tendency for the development of new grains will be discussed in detail in this section.

Based on the discussion in the previous section, we can assume that both the deformation heterogeneities that result in development of MSBs and the dynamic recovery are expected to play important roles in the grain refinement taking place during SPD. Temperature dependence of the factors controlling grain refinement during SPD for low- to moderately alloyed Al alloys is illustrated schematically by solid lines in Figure 15. It is known that the structural heterogeneity introduced by plastic deformation generally decreases with increase in deformation temperature. Because an increase in number of operating slip systems gives rise to more homogeneous deformation and also grain boundary sliding (GBS) can take place especially in the UFGed regions at high temperature and so result in a high rate of relaxation processes operating in matrices with heterogeneous microstructures. In addition, the deformed microstructure evolved at high temperatures becomes rather unstable because of frequent operation of dynamic restoration, such as dynamic recovery and even recrystallization. As a result, the fraction of grains having large-scale MSBs can be gradually decreased at elevated temperatures[34,36] and then fine-grained microstructures with HABs are hardly developed in original grains. Such temperature dependence of the probability of formation of MSBs is represented schematically in Figure 15 by a solid line 1. The solid line 2 in this figure shows in turn the relative potential for dynamic recovery to release the internal stresses evolved by plastic working, and promote the dislocation rearrangement in interiors of MSBs, resulting in the formation of perfect grain boundaries. It can be imagined[34] that the rate of dynamic recovery gradually increases with increasing temperature at $T \leq 0.5T_m$ and approaches a saturation at $T \gg 0.5T_m$, as shown in Figure 15. The overlap of the lines 1 and 2 can give a potential for development of strain-induced grain refinement in a wide temperature region, which is indicated by a bold solid line 3. According to this model, the development of UFG structure during cold and warm working should be strongly assisted by thermally activated processes and kinetics of grain refinement may be controlled mainly by

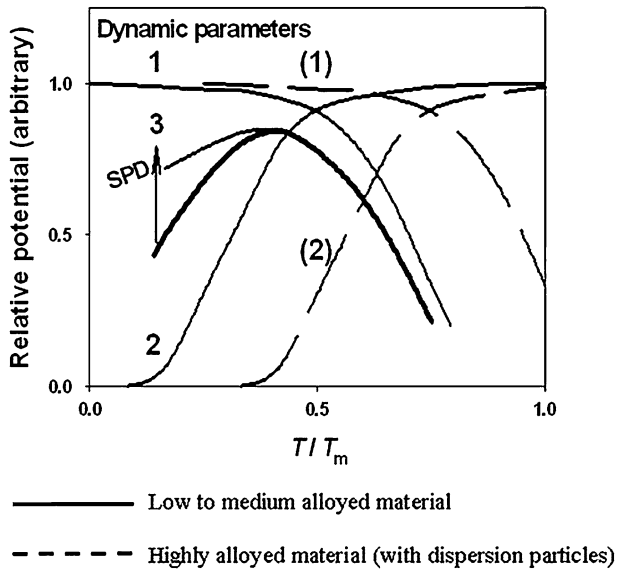

Fig. 15—Schematic representation for temperature dependence of various factors: 1—formation of MSBs, 2—dynamic recovery, and 3—overlapping effects of 1 and 2, controlling strain-induced grain formation taking place during SPD in a whole range of homologous temperatures ranging from 0 to 1.

the rate of dynamic recovery.[22] It has been shown[22,27] that SPD can remarkably accelerate diffusion/recovery processes operating over short distances and thus promote evolution of new grains even at relatively low temperatures from 0.14 to $0.35T_m$. At higher temperatures of above $0.5T_m$, in contrast, grain refinement can be mainly controlled by the possibility of development of MSBs which is normally decelerated with increasing temperature,[5,8,10,26,31] as discussed in Reference 40.

The above picture becomes much more complicated in the current highly alloyed Al-Mg-Sc alloy, in which all restoration processes are additionally inhibited by the presence of a large number of coherent dispersoid particles Al_3Sc (Figure 7) and also substitutional Mg atoms in solid solution.[23,24] These can effectively stabilize high-density dislocation microstructures and so MSBs evolved in such alloys can be more stable for a long period of processing time during hot ECAP.[23,24,29] On the other hand, an increasing deformation temperature may be very important for a rise in the misorientation of the deformation-induced dislocation subboundaries. It has been recently reported[16] that a strong inhibition of recovery takes place during ECAP of dispersoid-containing alloys and some Al-Mg alloys at ambient temperature. This makes MSBs more diffuse and represses their transformation into HABs. In contrast, increasing deformation temperature may give a greater possibility for the lattice dislocations to rearrange within the boundaries of MSBs to transform into permanent boundaries, which then increase their misorientation with further straining.[22,27] It is suggested, therefore, that both the solid lines 1 and 2 should be somewhat shifted toward higher temperatures in the case of highly alloyed materials, such as the present alloy with Mg and Sc additions, and can be shown by the dashed lines (1) and (2) in Figure 15. This suggests that kinetics of grain refinement in highly alloyed materials may be mainly controlled by the increasing rate of dynamic recovery and accelerated with raising temperature even during hot SPD.

Another factor that may retard the UFG structure evolution in the present alloy may be related with homogenization of dislocation slip due to a strong interaction of lattice dislocation with coherent dispersion particles and Mg atoms in solid solution.[16,30] The latter may provide a higher resistance to localization of plastic flow, as compared with some dilute or low-to-moderate alloyed Al alloys, and, hence, a lower density of MSBs can develop in the grain interiors during SPD.[30] This may be an additional reason why arrays of coarser fragments of original grains are frequently retained in the grain structure even after severe strains at 523 K (250 °C), resulting in a bimodal grain size distribution (Figures 5 and 9). In this way, increase in deformation temperature can promote more rapid transformation of such mixed structure into true fine-grained one through grain rotation.[17,30,34] Note that the Al-Mg-Sc alloy with an average grain size of about 1 μm exists stably and exhibits excellent superplastic properties in a wide strain rate interval at 723 K (450 °C).[41] When GBS takes place at a higher temperature, it may operate locally in fine-grained zones evolved along MSBs introduced by early deformation. This results in rotation of each fragmented region, *e.g.*, A and B in Figure 13, finally followed by in situ evolution of new grains with different crystallographic orientation, the size of which would be mainly controlled by the spacing of MSBs.[17] The speculation mentioned above is supported by the fact that rather strong texture developed at 523 K (250 °C) is changed to a roughly random one at 723 K (450 °C) (Figure 12). Under such conditions, by the way, only grain fragmentation by MSBs may be required for new grain structure in an early stage of SPD and so the kinetics of new grain formation should be much accelerated comparing with that for a full development of MSBs at lower temperatures.[30]

V. CONCLUSIONS

Microstructural evolution was examined in a commercial Al-6Mg-0.3Sc alloy, which was subjected by ECAP by route A to a total strain of 12 at 523 K (250 °C). The microstructural characteristics and the processes of new fine grain formation were analyzed and discussed comparing to those taking place at 723 K (450 °C). The main results can be summarized as follows.

1. Structural changes during warm-to-hot ECAP are associated with development of MSBs, which are continuously formed by strain accumulation and microstructural heterogeneities, resulting in fragmentation of coarse original grains.
2. UFGs with moderate-to-high angle boundary misorientations are concurrently evolved primarily at the intersections of MSBs and followed by their development in the interiors of MSBs accompanied by rigid body rotation at medium-to-larger strains.
3. Original grain subdivision mentioned in (1) along with simultaneous development of the UFG grains mentioned in (2) results in gradual development of macroscopically uniform regions with a mixed deformation structure, which contains coarser fragments of original grains bonded by the colonies of UFG grains. The microstructure developed at $\varepsilon = 12$ is characterized by a bimodal crystallite size distribution with two peaks at $d_1 \approx 0.2$ to 0.3 μm and $d_2 \approx 0.6$ to 0.7 μm, and the fraction of HABs of about 0.35 ± 0.05.
4. Dynamic formation of UFGed structure occurs very slowly and incompletely even at very high strains at 523 K (250 °C). This may result from slip homogenization and inhibition of recovery in the heavily alloyed Al alloy because of a strong interaction of lattice dislocations with coherent dispersion particles and also substitutional atoms in solid solution, which can make MSBs more diffuse and repress their transformation into HABs.
5. Kinetics of grain refinement is accelerated with increasing ECAP temperature from 523 K to 723 K (from 250 °C to 450 °C). Such positive temperature dependence of development of new UFGed

structure during warm-to-hot SPD in the present alloy is opposite to the results for conventional Al alloys with low-to-moderate concentration of alloying elements. This may result from the relative potentials for formation of MSBs and for dynamic recovery taking place during ECAP.

ACKNOWLEDGMENTS

This study was supported by the Ministry of Education and Science of Russian Federation under grant no. P1065.

REFERENCES

1. F.J. Humphreys, P.B. Prangnell, J.R. Bowen, A. Gholinia, and C. Harris: *Philos. Trans. R. Soc. Lond.*, 1999, vol. A357, pp. 1663–81.
2. Y. Saito, H. Utsunomiya, N. Tsuji, and T. Sakai: *Acta Mater.*, 1999, vol. 47, pp. 579–83.
3. R.Z. Valiev, R.K. Islamgaliev, and I.V. Alexandrov: *Prog. Mater. Sci.*, 2000, vol. 45, pp. 103–89.
4. C. Pithan, T. Hashimoto, M. Kawazoe, J. Nagahora K. Higashi: *Mater. Sci. Eng. A*, 2000, vol. 280, pp. 62–68.
5. A. Yamashita, D. Yamaguchi, Z. Horita, and T.G. Langdon: *Mater. Sci. Eng. A*, 2000, vol. 287, pp. 100–06.
6. A. Gholinia, P.B. Prangnell, and M.V. Markushev: *Acta Mater.*, 2000, vol. 48, pp. 1115–30.
7. Y.T. Zhu and T.C. Lowe: *Mater. Sci. Eng. A*, 2000, vol. 291, pp. 46–53.
8. U. Chakkingal and P.F. Thomson: *J. Mater. Process. Technol.*, 2001, vol. 117, pp. 169–77.
9. R.M. Imayev, G.A. Salishchev, O.N. Senkov, V.M. Imayev, M.R. Shagiev, N.K. Gabdullin, A.V. Kuznetsov, and F.H. Froes: *Mater. Sci. Eng. A*, 2001, vol. 300, pp. 263–77.
10. J.Y. Chang, J.S. Yoon, and G.H. Kim: *Scripta Mater.*, 2001, vol. 45, pp. 347–54.
11. A. Belyakov, T. Sakai, H. Miura, and K. Tsuzaki: *Philos. Mag.*, 2001, vol. A81, pp. 2629–43.
12. N. Tsuji, Y. Ito, Y. Saito, and Y. Minamino: *Scripta Mater.*, 2002, vol. 47, pp. 893–99.
13. J. Gibicza, N.Q. Chinh, Z. Horita, and T.G. Langdon: *Mater. Sci. Eng. A*, 2004, vols. 387–389, pp. 55–59.
14. Y.C. Chen, Y.Y. Huang, C.P. Chang, and P.W. Kao: *Acta Mater.*, 2003, vol. 51, pp. 2005–15.
15. O.V. Mishin, D. Juul Jensen, and N. Hansen: *Mater. Sci. Eng. A*, 2003, vol. 342, pp. 320–28.
16. P.J. Apps, M. Berta, and P.B. Pragnell: *Acta Mater.*, 2005, vol. 53, pp. 499–511.
17. O. Sitdikov, T. Sakai, A. Goloborodko, H. Miura, and R. Kaibyshev: *Philos. Mag.*, 2005, vol. 85, pp. 1159–75.
18. M. Popovic and B. Verlinden: *Mater. Sci. Technol.*, 2005, vol. 21, pp. 606–12.
19. J.C. Werenskiold and H.J. Roven: *Mater. Sci. Eng. A*, 2005, vols. 410–411, pp. 174–77.
20. R.Z. Valiev and T.G. Langdon: *Prog. Mater. Sci.*, 2006, vol. 51, pp. 881–981.
21. T.G. Langdon: *Mater. Sci. Eng. A*, 2007, vol. 462, pp. 3–11.
22. C. Kobayashi, T. Sakai, A. Belyakov, and H. Miura: *Philos. Mag. Lett.*, 2007, vol. 87, pp. 751–66.
23. O. Sitdikov, T. Sakai, E. Avtokratova, R. Kaibyshev, Y. Kimura, and K. Tsuzaki: *Mater. Sci. Eng. A*, 2007, vol. 444, pp. 18–30.
24. O. Sitdikov, T. Sakai, E. Avtokratova, R. Kaibyshev, K. Tsuzaki, and Y. Watanabe: *Acta Mater.*, 2008, vol. 56, pp. 821–34.
25. I. Mazurina, T. Sakai, H. Miura, O. Sitdikov, and R. Kaibyshev: *Mater. Sci. Eng. A*, 2008, vol. 473 (1–2), pp. 297–305.
26. I. Mazurina, T. Sakai, H. Miura, O. Sitdikov, and R. Kaibyshev: *Mater. Sci. Eng. A*, 2008, vol. 486, pp. 662–71.
27. T. Sakai, A. Belyakov, and H. Miura: *Metall. Mater. Trans. A*, 2008, vol. 39A, pp. 2206–14.
28. R.R. Mulyukov, R.M. Imayev, and A.A. Nazarov: *J. Mater. Sci.*, 2008, vol. 43, pp. 7257–63.
29. O. Sitdikov, E. Avtokratova, T. Sakai, K. Tsuzaki, R. Kaibyshev, and Y. Watanabe: *Mater. Sci. Forum*, 2008, vols. 584–586, pp. 481–86.
30. O. Sitdikov, T. Sakai, H. Miura, and C. Hama: *Mater. Sci. Eng. A*, 2009, vol. 516, pp. 180–88.
31. I. Mazurina, T. Sakai, H. Miura, O. Sitdikov, and R. Kaibyshev: *Mater. Trans.*, 2009, vol. 50 (1), pp. 101–10.
32. Y.J. Chen, H.J. Roven, S.S. Gireesh, P.C. Skaret, and J. Hjelen: *Mater. Lett.*, 2011, vol. 65, pp. 3472–75.
33. Y.J. Chen, Y.C. Chai, H.J. Roven, S.S. Gireesh, Y.D. Yu, and J. Hjelen: *Mater. Sci. Eng. A*, 2012, vol. 545, pp. 139–47.
34. F.J. Humphreys and M. Hatherly: *Recrystallization and Related Annealing Phenomena*, 2nd ed., Elsevier, Amsterdam, 2004, p. 658.
35. O. Sitdikov and R. Kaibyshev: *Mater. Sci. Eng. A*, 2002, vol. 328, pp. 147–55.
36. E. Ball and F.J. Humphreys: *Thermomechanical Processing in Theory, Modeling and Practice (TMP²)*, ed. by B. Hutchinson, M. Andersson, T. Siwecki, B. Karlsson, and G. Engberg, Stockholm (1996), ASM Inter., 1997, pp. 184–92.
37. A. Duckham, R.D. Knutsen, and O. Engler: *Acta Mater.*, 2001, vol. 49, pp. 2739–49.
38. U.F. Kocks, C.N. Tome, and H.R. Wenk: *Texture and Anisotropy*, Cambridge University Press, Cambridge, UK, 1998, p. 195.
39. P.J. Hurley and F.J. Humphreys: *Acta Mater.*, 2003, vol. 51, pp. 1087–102.
40. T. Sakai and H. Miura: *Mater. Sci. Forum*, 2012, vols. 706–709, pp. 1829–34.
41. F. Musin, R. Kaibyshev, Y. Motohashi, and G. Itoh: *Metall. Mater. Trans. A*, 2004, vol. 35A, pp. 2383–92.